Human umbilical cord mesenchymal stem cell-derived exosomal miR-214-3p regulates the progression of gallbladder cancer by regulating ACLY/GLUT1

Luyao Liu[1,A,B,D,F], Wang Xiao[2,B,C,E,F], Zhulin Yang[2,B,C,F], Qunwei Wang[2,A,C,F], Jianing Yi[3,A,C,E,F]

[1] Department of General Surgery, Hunan Provincial People's Hospital, The First Affiliated Hospital of Hunan Normal University, Changsha, China
[2] Department of General Surgery, The Second Xiangya Hospital of Central South University, Changsha, China
[3] Department of Breast and Thyroid Gland Surgery, Hunan Provincial People's Hospital, The First Affiliated Hospital of Hunan Normal University, Changsha, China

A – research concept and design; B – collection and/or assembly of data; C – data analysis and interpretation;
D – writing the article; E – critical revision of the article; F – final approval of the article

Advances in Clinical and Experimental Medicine, ISSN 1899–5276 (print), ISSN 2451–2680 (online) *Adv Clin Exp Med*. 2024;33(5):499–510

Address for correspondence
Jianing Yi
E-mail: yijianing@hunnu.edu.cn

Funding sources
None declared

Conflict of interest
None declared

Received on November 11, 2022
Reviewed on February 14, 2023
Accepted on July 24, 2023

Published online on September 25, 2023

Abstract

Background. Human umbilical cord mesenchymal stem cell (hucMSC)-derived exosomes have been reported to be effective in the treatment of cancer. The miR-214-3p is a suppressor miRNA that has been extensively studied and has been proposed as a diagnostic and prognostic biomarker in some cancers.

Objectives. The aim of this study was to investigate whether the regulatory mechanism of hucMSC-derived exosomal miR-214-3p with GLUT1 and ACLY affects the proliferation and apoptosis of gallbladder cancer (GBC) cells.

Materials and methods. We found that the target genes of miR-214-3p on the TargetScan website contain GLUT1 and ACLY, and the targeting relationship was verified using luciferases. The GBC-SD cells overexpressing GLUT1 and ACLY were constructed to determine proliferation, apoptosis, migration, and other cellular activities.

Results. We identified hucMSCs and exosomes, and found that the exosomes contained miR-214-3p. Furthermore, TargetScan predicted that miR-214-3p had base interactions with ACLY. Dual luciferase assays showed that miR-214-3p could inhibit ACLY ($p < 0.05$). The results of quantitative reverse transcription polymerase chain reaction (RT-qPCR) and western blot showed that exosomal miR-214-3p could inhibit the expression of ACLY and GLUT1 ($p < 0.05$). Exosomal miR-214-3p can inhibit the proliferation, cloning and migration of GBC-SD cells ($p < 0.05$). The apoptosis of GBC-SD cells was increased ($p < 0.05$). The GBC-SD cells overexpressing ACLY and GLUT1 could reverse the efficacy of miR-214-3p.

Conclusions. Exosomal miR-214-3p can inhibit the downstream expression of ACLY and GLUT1. The ACLY and GLUT1 could affect the proliferation and apoptosis of GBC-SD cells.

Key words: GLUT1, exosomes, miR-214-3p, ACLY

Cite as
Liu L, Xiao W, Yang Z, Wang Q, Yi J. Human umbilical cord mesenchymal stem cell-derived exosomal miR-214-3p regulates the progression of gallbladder cancer by regulating ACLY/GLUT1. *Adv Clin Exp Med*. 2024;33(5):499–510. doi:10.17219/acem/169976

DOI
10.17219/acem/169976

Background

Gallbladder cancer (GBC) is an uncommon human malignancy that has a particular geographical distribution in Central and South America, Central and Eastern Europe, Japan, and Northern India.[1,2] It is on the rise globally and its prognosis is very poor. Since GBCs are usually asymptomatic, early diagnosis may not be possible.[3] Clinical evidence indicates that many GBC patients are diagnosed as inoperable, a state at which the tumor has already become invasive and metastatic.[4] The overall prognosis of GBC is extraordinarily poor and the mean survival ranges from 13.2 to 19 months.[5] Although some prognostic biomarkers in adenosquamous carcinoma (ASC) have shown some promise, the clinical use of these proposed biomarkers has not yet been approved.[6,7] Currently, there are no reliable or acceptable molecular markers associated with simple cholecystectomy (SC) or ASC progression and prognosis.

During oncogenesis, the metabolism of a tumor cell is reprogrammed to support rapid proliferation of tumor cells.[8] Previous studies have reported that many metabolic genes play a significant role in the progression of cancer, and can be used as putative biomarkers for prognosis and targets for therapeutic agents. The basic metabolic processes of tumor cells are glycolysis and lipogenesis. It was discovered that most fatty acids in cancer come from lipogenesis.[9] Glycolysis is a biochemical process. In cancer cells, adenosine triphosphate (ATP) is the main energy source.[10] Moreover, the fatty acids synthesized in the process of adipogenesis are used as the main fuel for the rapid proliferation of cancer cells to produce cell membranes.[11] At present, at least 5 genes in the glycolysis and lipogenesis pathways are directly involved in tumorigenesis and tumor progression. The GLUT1 promotes increased glucose transport in tumor cells and maintains a high glycolysis rate in aerobic conditions. However, ACLY can convert citrate into acetyl-CoA for fat generation as a cell solute enzyme.[9] Therefore, GLUT1 and ACLY are known as key enzymes in the rate-limiting first step of the metabolic pathway. In various tumors, such as breast cancer,[12,13] colorectal cancer,[14,15] gastric cancer,[16,17] hepatocellular cancer,[18,19] and prostate cancer,[20–22] GLUT1 and ACLY are upregulated. In this regard, we further explored whether GLUT1 and ACLY play a role in the life activities of cholangiocarcinoma cells.

The human umbilical cord mesenchymal stem cell (hucMSC)-derived exosomes (hucMSC-exo) exert anti-inflammatory effects on human trophoblastic cells by transferring miRNAs.[23] The miR-214 was reported to be a member of a vertebrate-specific miRNA precursor involved in regulating glucose metabolism in the liver.[24] It also has an important role in skeletal diseases.[25] The miR-214-3p is a suppressor miRNA that has been extensively studied and has been proposed as a diagnostic and prognostic biomarker in some cancers.[26]

Objectives

Therefore, the aim of the study was to investigate whether the regulatory mechanism of miR-214-3p with GLUT1 and ACLY affects the proliferation and apoptosis of GBC cells.

Materials and methods

Cell transfection

Human gallbladder carcinoma GBC-SD cells (BNCC100091) were purchased from Beina Biological Co., Ltd. (Beijing, China). The required si-RNA-negative control (NC), si-GLUT1 and si-ACLY were removed, and ice thawing was performed. Two of the 8 sterile centrifuges were taken, and 95 µL of serum-free 1640 medium was added to each tube. Then, 5 µL of i-RNA-NC and 5 µL of Lipofectamine 2000 were added to the centrifuges, respectively. Another si-RNA was added to the corresponding centrifuge tube in the same way. The mixture was gently mixed and left to stand for 5 min at room temperature. Then, the 2 tubes were gently mixed and left to stand for 20 min at room temperature. Finally, the mixture was evenly added to the wells to be transfected and mixed. All plasmids were purchased from HonorGene Company (Changsha, China).

Separation of exosomes

The hucMSCs were obtained from the umbilical cord tissue of newborns. Five cell surface markers (CD105, CD90, CD34, CD14, and CD166) were evaluated to identify hucMSCs. The hucMSCs were counted to ensure that each cell suspension had more than 1×10^6 cells. The cells were incubated with human anti-CD105 (P-phycoerythrin (PE)), anti-CD90 (PE), anti-CD34 (PE), anti-CD14 (fluorescein isothiocyanate (FITC)), and anti-CD166 (FITC) (all from eBioscience, San Diego, USA), respectively, for 30 min at room temperature. Then, the cells were washed and suspended for flow cytometry analysis. Half the volume of an exosome separation solution was added to the supernatant, blown, mixed, and placed in the refrigerator at 4°C overnight. After 12 h, the supernatant was centrifuged for 1 h at 4°C. The supernatant solution was discarded, and the precipitate was retained. The precipitate was blown with phosphate-buffered saline (PBS) and fully mixed to form an exosome suspension. The concentration of exosomes was detected with bicinchoninic acid (BCA) protein concentration and stored at –80°C as reserve. The effective storage time of exosomes was 1 month.

Identification of exosomes

The exosomes were identified with transmission electron microscopy (TEM) (TecnaiTM G2 Spirit BIOTWIN; Thermo Fisher Scientific, Waltham, USA). A volume

of 20 µL of exosomes was dropped onto the copper mesh and left for 3 min. The cells were dried with an incandescent lamp, and pictures were taken under the TEM. The particle size analysis was performed using a nanoparticle tracking analysis (NS300; Malvern Panalytical, Malvern, UK). Western blot was utilized to identify the surface markers of exosomes. The protein content of the exosome suspension was measured with the use of a BCA kit (23227; Thermo Fisher Scientific), the sodium dodecyl-sulfate polyacrylamide gel electrophoresis (SDS-PAGE) gel was prepared, protein denaturation and electrophoresis were performed, and the membrane was transferred to detect the exosome-specific marker protein HSP70 (ab5439, 1:1000), CD63 (ab134045, 1:2000), CD81 (ab79559, 1:1000), and calnexin (ab22595, 1 µg/mL; Abcam, Cambridge, UK).

Alizarin red S assay

Oligodendrocyte Medium (OM) was used to culture 2×10^4 cells for 7 days. Then, the cells were stained with alizarin red and quantitatively analyzed. A nitrotetrazolium Blue chloride (NBT)/5-Bromo-4-chloro-3-indolyl phosphate (BCIP) staining kit (72091; MilliporeSigma, St. Louis, USA) was used for alizarin red staining after cell fixation. The alizarin red Active Colorimetric Quantitative Detection Kit was purchased from Nanjing Jiancheng Reagent Company (Nanjing, China). Depending on the instructions, the cells were collected, separated at 1000 rpm for 10 min, and observed with Triton-X100 or X400. The optical density (OD) of cells was measured at 520 nm. The experiment was repeated 3 times.

Oil Red O staining

Modified Oil Red O staining solution was used to stain 2×10^4 cells for 10–15 min in airtight conditions, protected from light. Mayer's hematoxylin staining solution was added to remove the stain, and the nuclei were restained for 5 min. The slices were blotted with filter paper and sealed with glycerol gelatin or gum arabic.

RT-qPCR

Total RNA was extracted from brain tissues using Trizol (15596026; Thermo Fisher Scientific).

About 500 µL of GBC-SD cells were collected into a new 1.5-mL centrifuge tube, and Trizol was supplemented to 1 mL after mixing, followed by chamber lysis for 3 min. Next, 200 µL of trichloromethane were added into the centrifuge tube, the tube was shaken vigorously for 15 s and then stood at room temperature for 3 min. The concentration was determined with a ultraviolet (UV) spectrophotometer, the absorbance (OD) value was measured at 260 nm and 280 nm, and the concentration and purity were calculated. Vortex oscillation mixing and temporary centrifugation were used for the wall of the solution to be collected at the bottom of the tube. The solution was incubated for 50 min at 50°C and 5 min at 85°C. Reaction conditions were as follows: 40 cycles of pre-denaturation at 95°C for 10 min, denaturation at 94°C for 15 s and annealing at 60°C for 30 s. After the reaction, the tubes were briefly centrifuged and cooled on ice. The internal reference primer was β-actin. The primer sequences are presented in Table 1. With 2 µg cDNA as template, the $2^{-\Delta\Delta Ct}$ relative quantitative method was used. The relative transcription level of the target gene was calculated as follows (Equation 1,2):

Table 1. Primer sequences

Gene	Sequence (5′-3′)
miR-214-3p	F: CTGGCTGGACAGAGTTGTCAT
	R: GCTGTACAGGTGAGCGGATG
GLUT1	F: CTATGGGGAGAGCATCCTGC
	R: CCCAGTTTCGAGAAGCCCAT
ACLY	F: CCTCAGCCATCCAGAATCGG
	R: CTTCAGCCAGGACTTGACCC
β-actin	F: ACCCTGAAGTACCCCATCGAG
	R: AGCACAGCCTGGATAGCAAC
U6	F: CTCGCTTCGGCAGCACA
	R: AACGCTTCACGAATTTGCGT

$$\Delta\Delta Ct = \Delta \text{ experimental group} - \Delta \text{ control group} \quad (1)$$

$$\Delta Ct = Ct \text{ (target gene)} - Ct \text{ (β-actin)} \quad (2)$$

Western blot

The GBC-SD cells were extracted using the Total Protein Extraction Solution RIPA kit (R0010; Beijing Solarbio Science & Technology Co., Ltd., Beijing, China). For primary antibodies, we used rabbit anti-p-mTOR (1:5000, ab109268), mouse anti-mTOR (1:10000, 66888-1-Ig), mouse t anti-p-AKT (1:5000, 66444-1-Ig), rabbit anti-AKT (1:1000, 10176-2-AP), rabbit anti-p-PI3K (0.5 µg/m, ab278545), mouse anti-PI3K (1:800, 67071-1-AP), mouse anti-Bax (1:10000, 60267-1-AP), mouse anti-Bcl-2 (1:1000, 60178-1-AP), rabbit anti-caspase 3 (1:5000, #9661, CST0), and mouse anti-β-actin (1:5000, 66009-1-Ig). All antibodies were purchased from Proteintech Genomics (San Diego, USA). The membrane was immersed in Superecl Plus (k-12045-d50, Advansta, USA) for the development of luminescence. The β-actin was used as an internal reference. Image J software (NIH, USA) was utilized to analyze gray values.

CCK-8

Cells in each group were counted and inoculated into 96-well plates at a density of 5×10^3 cells/well, 100 µL per well. Each group was equipped with 3 multiple holes. After culture and adherence, the treatment was carried

out in accordance with the above method. After the corresponding time, 10 μL of Cell Counting Kit-8 (CCK-8) (NU679; Dojindo Laboratories, Kumamoto, Japan) was added to each well, and the CCK-8 solution was prepared with a complete medium. Then, the drug-containing medium was removed and 100 μL of CCK-8 medium was added to each well. The OD value at 450 nm was analyzed using the BioTek microplate analyzer (DSZ2000X; Cnmicro, Beijing, China) after further incubation at 37°C for 4 h at 5% CO_2, and the mean value was drawn as a histogram.

Wound healing assay

A flask of cells was taken and trypsinized, and after counting, approx. 5×10^5 cells were added to each well. After the cells were covered with the plate, the pipette tip was used to draw a horizontal line perpendicular to the previously drawn horizontal line. Cells were washed 3 times with sterile PBS, streaked cells were removed, and serum-free 1640 medium (R8758; Sigma-Aldrich, St. Louis, USA) was added. The scratches were photographed at 0 h, and 3 fields of view were taken at each timepoint. After culturing at 37°C and 5% CO_2 for 24 h and 48 h, pictures were taken again for recording.

Double luciferase activity

The target gene analysis of ACLY with miR-214-3p was performed using TargetScan website (https://www.targetscan.org/vert_80) to verify whether there is a targeting relationship between ACLY and miR-214-3p using the luciferase reporter gene assays. The target gene ACLY dual luciferase reporter gene vector and mutants with mutations of the binding site of miR-214-3p (pGL3-ACLY Wt and pGL3-ACLY Mut) were constructed, respectively. Two reporter plasmids were co-transfected with the overexpression of miR-214-3p into cells, and 24 h after transfection, the cells were lysed according to the TransDetect® Double-Luciferase Reporter Assay Kit procedure (FR201-01; full-form gold; Antipedia, Beijing, China), and the supernatant was collected. After that, 100 μL of luciferase reporter gene activity (Renilla luciferase) was added to Reaction Reagent II and the ratio of firefly luciferase to sea kidney luciferase (FL/RL) was used to determine relative luciferase activity. Each experiment was repeated 3 times.

Cell colony formation

Cells from each group of the p-index growth phase were taken, digested with 0.25% trypsin, blown into individual cells, and suspended in a complete medium with 10% calf serum. The cells were incubated at 37°C in 5% CO_2 and saturated humidity for 2–3 weeks, with appropriate fluid changes. The culture medium was discarded, and the PBS solution (SH30256.01; HyClone, Logan, USA) was carefully washed twice. The 6-well plate was removed and soaked with 1 mL of 10% acetic acid to decolorize. The absorbance was measured at 450 nm using a microplate reader (MB-530; Huisong Pharmaceuticals, Hangzhou, China).

Flow cytometry analysis

The cells were collected using digestion with ethylenediaminetetraacetic acid (EDTA)-free trypsin. They were washed twice with PBS and centrifuged at 2000 rpm for 5 min each time to collect approx. 3.2×10^5 cells. Next, 500 μL of binding buffer was added to suspend the cells. After adding 5 μL of Annexin V-APC, 5 μL of propidium iodide (MBC0409; Meilunbio, Wuhan, China) was added, mixed at room temperature and protected from light. The reaction was performed for 10 min within 1 h and detected with flow cytometry.

The fixed sample was taken out, centrifuged at 800 rpm for 5 min, and the supernatant was discarded. Then, 1 mL of pre-cooled PBS was added to resuspend the cells, centrifuged at 800 rpm for 5 min, and the cells were collected by centrifugation. Next, 150 μL of propidium iodide working solution was added and stained at 4°C for 30 min in the dark. The percentage of each cell cycle on the fluorescence histogram was analyzed.

Transwell assay

The cells treated above were digested with trypsin to form single cells, resuspended in serum-free medium to 2×10^6 cells/mL, and 100 μL of cells were added to each well. The upper chamber was taken out and placed in a new well containing PBS. The pore size was 8 μm. The samples were stained with 0.1% crystal violet (G1062; Beijing Solarbio Science & Technology Co., Ltd.) for 5 min, washed with water 5 times, placed on a glass slide, and photographed under a microscope (model DSZ2000X; Cnmicro). The cells on the outer surface of the upper chamber were observed under an inverted microscope (model DSZ2000X; Cnmicro), and 3 fields of view were taken for each. The chamber was taken out and soaked in 500 μL of 10% acetic acid to decolorize, and the OD value was measured with a microplate reader (DSZ2000X; Cnmicro) at 550 nm.

Statistical analyses

All measurement data were expressed as mean ± standard deviation (M ±SD). The data were analyzed using GraphPad Prism v. 8.0 software (GraphPad Software, San Diego, USA). The Shapiro–Wilk test and F-test were used to compare variances and to evaluate whether the data conformed to a normal distribution and homogeneity of variance assumption. The unpaired Student's t-test was used to compare the data between 2 groups that did not have one-to-one correspondence. The Shapiro–Wilk test and the Brown–Forsythe test were used to analyze whether the data conformed to a normal distribution and

homogeneity of variance assumption. One-way analysis of variance (ANOVA) and Tukey's post hoc test were used to compare data among 3 groups. The measurement data obeyed the normal distribution and homogeneity of variance. The degrees of freedom and p-values for normal distribution were used to present the results of the analysis. The difference was statistically significant at $p < 0.05$.

Results

Identification of hucMSCs and exosomes

First, we performed cultures on the purchased hucMSCs. The cells showed shuttle-shaped, swirling growth (Fig. 1A). Flow cytometry was used to detect the cell surface antigens CD14 (0.80%), CD34 (0.54%), CD90 (98.76%), CD105 (96.01%), and CD166 (97.03%) (Fig. 1B). The hucMSCs showed osteogenic capacity (Fig. 1C) and lipogenic capacity (Fig. 1D). Transmission electron microscopy was used to observe the secretion of exosomes by huc-MSCs (TecnaiTM G2 Spirit BIOTWIN; Thermo Fisher Scientific). Exosomes were collected and were positive for exosome markers CD63, CD81 and HSP70, and negative for calnexin and elevated miR-214-3p expression (Fig. 1E–G). All raw data are presented in Supplementary Table 1. In short, hucMSCs can secrete exosomal miR-214-3p.

Exosomal miR-214-3p can affect the proliferation of GBC-SD

The above results indicated the presence of miR-214-3p in hucMSC exosomes. To investigate the effect of exosomal miR-214-3p on the development of cholangiocarcinoma,

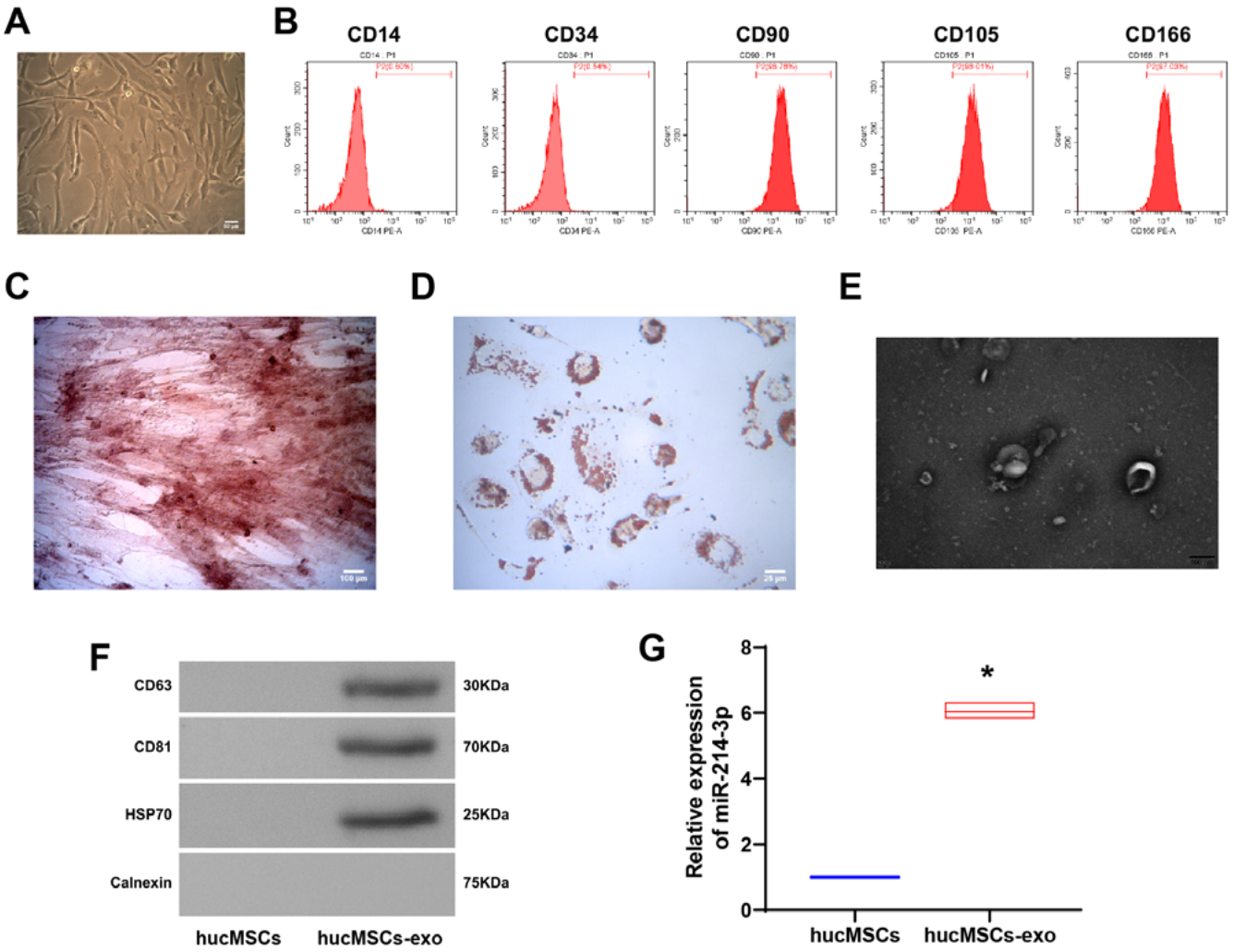

Fig. 1. Human umbilical cord mesenchymal stem cells (hucMSCs) can secrete exosomes. A. Fibrous appearance of hucMSCs; B. The ratio of markers indicates that the cells are hucMSCs; C. Alizarin red staining was used to observe the osteogenic ability of induced hucMSCs; D. Oil Red O staining was utilized to observe the ability to induce lipogenesis in hucMSCs; E. Transmission electron microscopy (TEM) recording of exosome images; F. Western blotting was used to detect hucMSC-derived exosomes (hucMSCs-exo) – CD63, HSP70, CD81, and calnexin; G. Quantitative reverse transcription polymerase chain reaction (RT-qPCR) was utilized to detect miR-214-3p expression in the hucMSC group and hucMSCs-exo group. The unpaired t-test was used to analyze comparisons between the 2 groups (n = 3)

*$p < 0.05$ compared to hucMSCs.

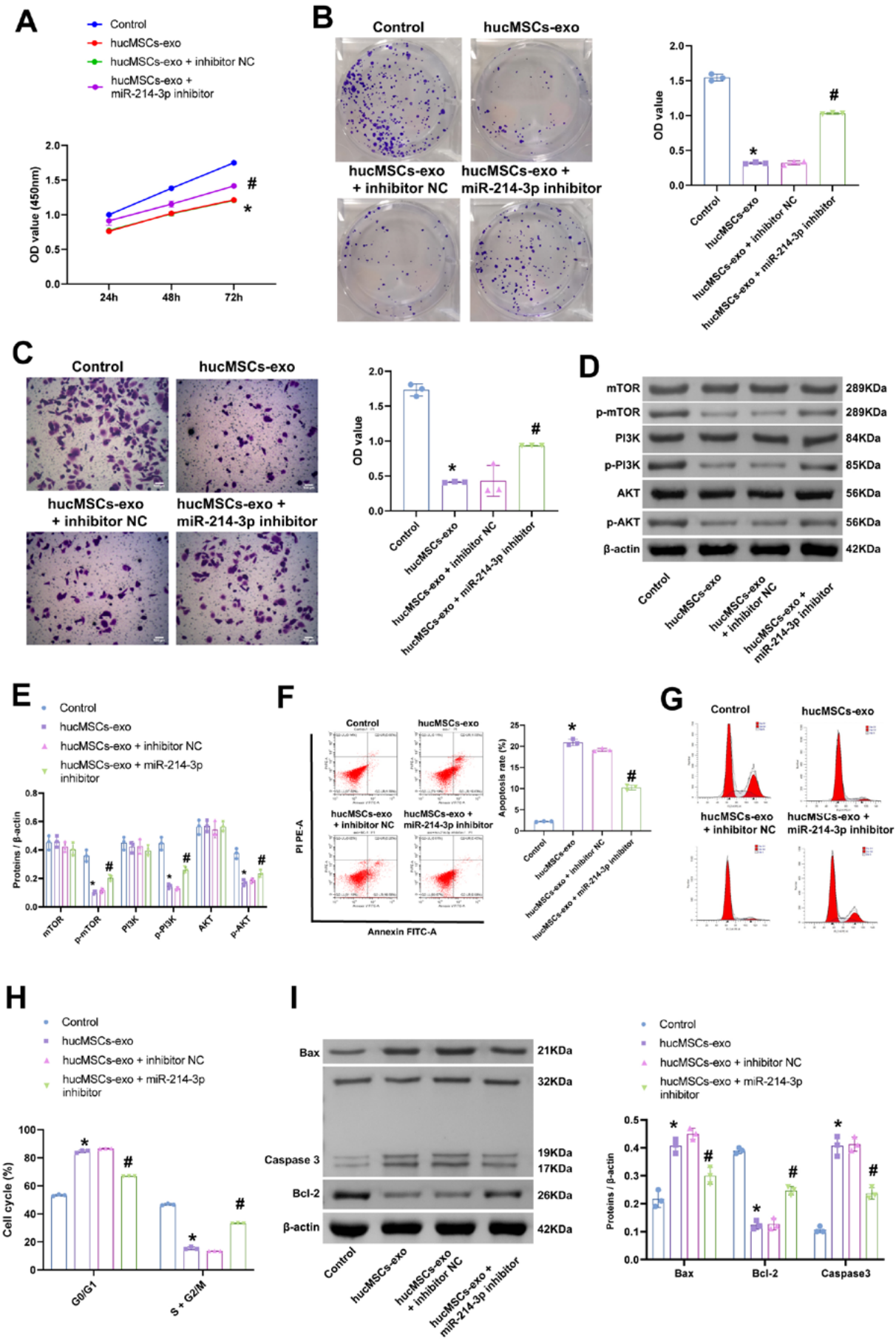

Fig. 2. Exosomal miR-214-3p can inhibit the proliferation of GBC-SD cells. A. Cell Counting Kit-8 (CCK-8) assays of GBC-SD cell proliferation at 24 h, 48 h and 72 h; B. Colony formation of GBC-SD cell clonal cell numbers; C. Transwell detection of GBC-SD cell invasion number; D,E. Western blot detection of proliferation-related pathway proteins (mTOR, p-mTOR, PI3K, p-PI3K, AKT, and p-AKT); F. Flow cytometry was used to detect the apoptosis rate of GBC-SD cells; G,H. Flow cytometry was utilized to detect the cycle of GBC-SD cells; I. The level of proteins (Bax, Bcl-2 and caspase 3). The comparisons among multiple groups were analyzed using one-way analysis of variance (ANOVA), followed by Tukey's post hoc test (n = 3)

*p < 0.05 compared to controls; #p < 0.05 compared to human umbilical cord mesenchymal stem cells (hucMSCs); OD – optical density; NC – negative control; GBC – gallbladder cancer; hucMSCs-exo – hucMSCs-derived exosomes.

the GBC-SD cell line was selected for subsequent experiments. The addition of exosomes in GBC-SD resulted in a decrease in cell proliferation (Fig. 2A), clonogenic ability (Fig. 2B), invasive ability (Fig. 2C), and an increase in the percentage of apoptosis (Fig. 2F) and G0/G1 phase (Fig. 2G,H). In contrast, after miR-214-3p silencing in GBC-SD, the proliferative, clonogenic and invasive capacities of the cells significantly increased after the addition of the exosomes in GBC-SD, while the percentage of apoptosis and S-phase decreased. The levels of p-mTOR, p-PI3K, p-AKT (Fig. 2D,E), and Bcl-2 decreased, and the expression of Bax and caspase 3 increased under exosome intervention. Silencing of miR-214-3p increased the levels of p-mTOR, p-PI3K, p-AKT, and Bcl-2, and inhibited the expression of Bax and caspase 3 (Fig. 2I). The data displayed in Fig. 2 are also presented in Supplementary Table 2. In short, miR-214-3p in exosomes was able to inhibit the proliferation of GBC-SD cells.

Exosomal miR-214-3p can regulate ACLY/GLUT1 to affect GBC-SD cells

The above experiments demonstrated that miR-214-3p can affect the proliferation and apoptosis of GBC-SD cells in exosomes. To investigate whether miR-214-3p can regulate the progression of GBC through ACLY/GLUT1, we constructed cell models overexpressing ACLY and GLUT1. The miR-214-3p expression levels were not affected by the overexpression of ACLY and GLUT1. Exosomal miR-214-3p inhibited ACLY and GLUT1 expression (Fig. 3A,B). The miR-214-3p was shown to have base interactions on the TargetScan website (https://www.targetscan.org/; Fig. 3C). Dual luciferase activity assays showed that miR-214-3p can target and inhibit the expression of ACLY (Fig. 3D). The data showed that exosome-competent miR-214-3p inhibited the proliferation of GBC-SD cells (Fig. 3E) and promoted their apoptosis (Fig. 3E), while the overexpression of ACLY and GLUT1 cells reversed this effect. The source data and analysis results of Fig. 3 are presented in Supplementary Table 3. In short, ACLY and GLUT1 can affect the proliferation and apoptosis of GBC-SD cells.

Inhibition of GLUT1 and ACLY can affect the proliferation of GBC-SD cells

The above results showed that GLUT1 and ACLY were associated with the prognosis of GBC patients. We planned to investigate whether GLUT1 and ACLY could affect the function of GBC-SD in vitro. Firstly, we constructed GBC-SD cells with the silencing of GLUT1 and ACLY. The data presented in Fig. 4A showed that the expression of GLUT1 and ACLY was inhibited in GBC-SD cells after silencing, indicating that the cell model was successfully constructed. Compared with the control and si-NC groups, the proliferative and clonogenic abilities of GBC-SD cells were reduced in the si-GLUT1 and si-ACLY groups, and the proliferative and clonogenic abilities of GBC-SD cells were more significantly reduced in the si-GLUT1+si-ACLY group (Fig. 4B–D). Then, we examined the expression of proliferation-related genes, and the expression of p-mTOR, p-PI3K and p-AKT was significantly reduced in GBC-SD cells silenced with GLUT1 and ACLY (Fig. 4E). The results of the data analysis displayed in Fig. 4 are presented in Supplementary Table 4. In short, silencing of GLUT1 and ACLY inhibited the proliferative capacity of GBC-SD cells.

Inhibition of GLUT1 and ACLY can affect GBC-SD cell migration

The above results suggested that GLUT1 and ACLY can affect the proliferation of GBC-SD cells, thus whether silencing GLUT1 and ACLY can inhibit the proliferation of GBC-SD cells required further study. Transwell assays were used to detect the migration and invasion ability of GBC-SD cells. The experimental results demonstrated that the migration and invasion ability of GBC-SD cells were reduced in the si-GLUT1 and si-ACLY groups compared to the control and si-NC groups, and the reduction of migration and invasion ability of GBC-SD cells was more significant in the si-GLUT1+si-ACLY group (Fig. 5A,B). The scratch assays were performed to measure the migration distance, and the migration distance of GBC-SD cells silenced with GLUT1 and ACLY was significantly lower (Fig. 5C). The results displayed in Fig. 5 are presented in Supplementary Table 5. In conclusion, silencing of GLUT1 and ACLY inhibited the migratory ability of GBC-SD cells.

Inhibition of GLUT1 and ACLY can affect the apoptosis of GBC-SD cells

The above results suggested that GLUT1 and ACLY can affect the proliferation and migration of GBC-SD cells; thus, whether the silencing of GLUT1 and ACLY can promote apoptosis of GBC-SD cells required further investigation. Flow cytometry was used to detect the apoptosis rate of GBC-SD cells. Compared to the control and si-NC groups, the apoptosis rate of GBC-SD cells was elevated in the si-GLUT1 and si-ACLY groups, and the increase in the GBC-SD cell apoptosis rate was more significant in the si-GLUT1+si-ACLY group (Fig. 6A). The results of the data in Fig. 6B showed that the sum of S and G2/M phases of GBC-SD cells in the si-GLUT1 and si-ACLY groups were decreased compared to the control and si-NC groups, and the sum of S and G2/M phases of GBC-SD cells in the si-GLUT1+si-ACLY group was decreased more significantly. Western blot was utilized to analyze the expression of apoptosis-related proteins. The expression of Bax and caspase 3 was significantly increased, while the expression of Bcl-2 was significantly decreased in GBC-SD cells silenced with GLUT1 and ACLY (Fig. 6C). The results displayed in Fig. 6 are presented in Supplementary Table 6. All in all, silencing of GLUT1 and ACLY promoted apoptosis in GBC-SD cells.

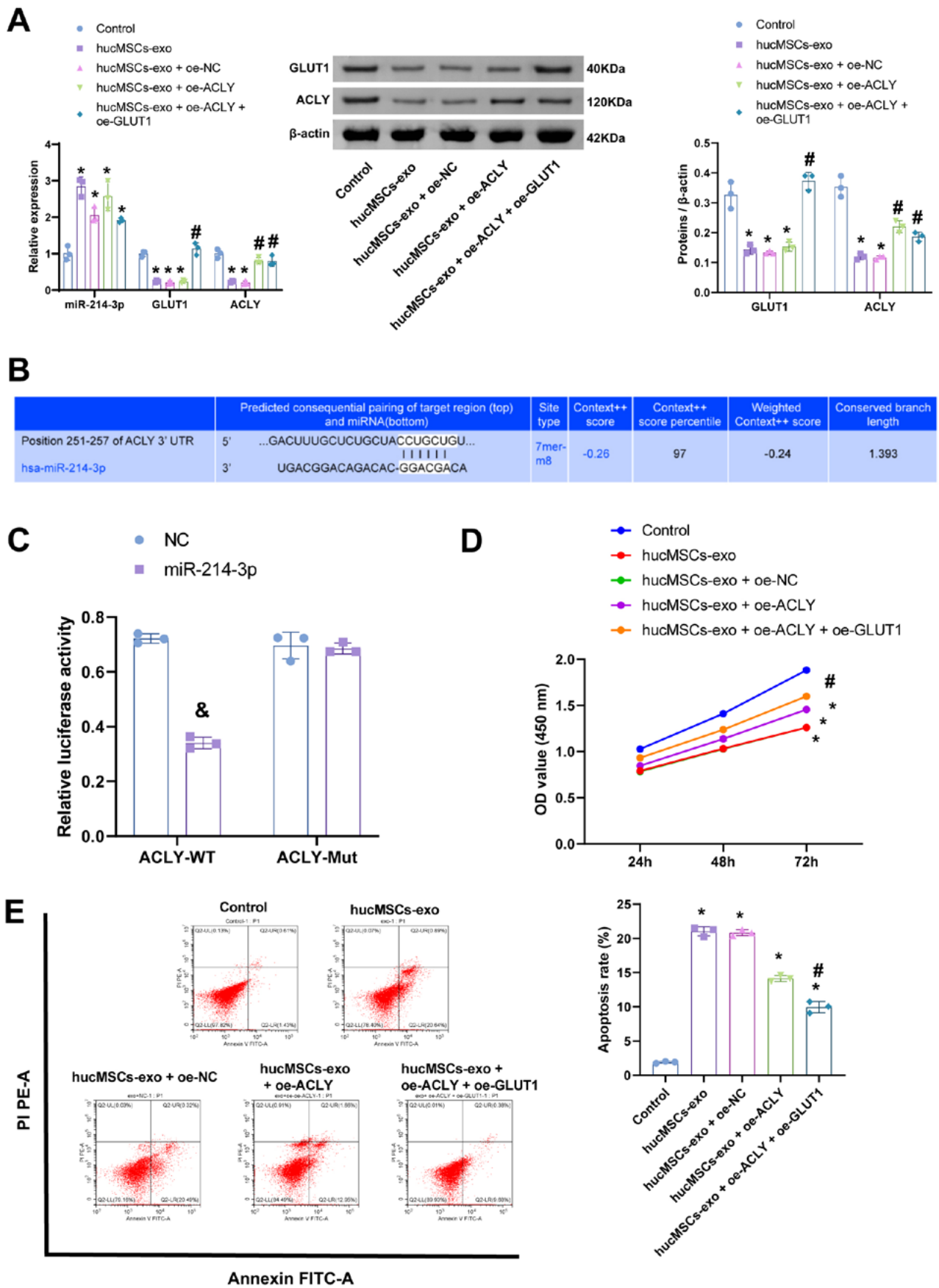

Fig. 3. Exosomal miR-214-3p can affect ACLY/GLUT1 to inhibit the proliferation of GBC-SD cells. A. Quantitative reverse transcription polymerase chain reaction (RT-qPCR) was used to detect the expression of miR-214-3p, GLUT1 and ACLY in the 2 groups, and Western blot was used to detect GLUT1 and ACLY; B. StarBase website predicted a targeting relationship between miR-214-3p and ACLY; C. Dual luciferase detection of miR-214-3p targeted inhibition of ACLY expression; D. Cell Counting Kit-8 (CCK-8) was used to detect the proliferation of GBC-SD cells at 24 h, 48 h and 72 h; E. Flow cytometry was used to analyze the apoptosis rate of GBC-SD cells. The unpaired t-test was used to analyze comparisons between 2 groups, and the comparisons among multiple groups were analyzed using one-way analysis of variance (ANOVA), followed by Tukey's post-hoc test (n = 3)

*p < 0.05 compared to controls; #p < 0.05 compared to human umbilical cord mesenchymal stem cells (hucMSCs); &p < 0.05 compared to NC; OD – optical density; NC – negative control; GBC – gallbladder cancer; hucMSCs-exo – hucMSCs-derived exosomes.

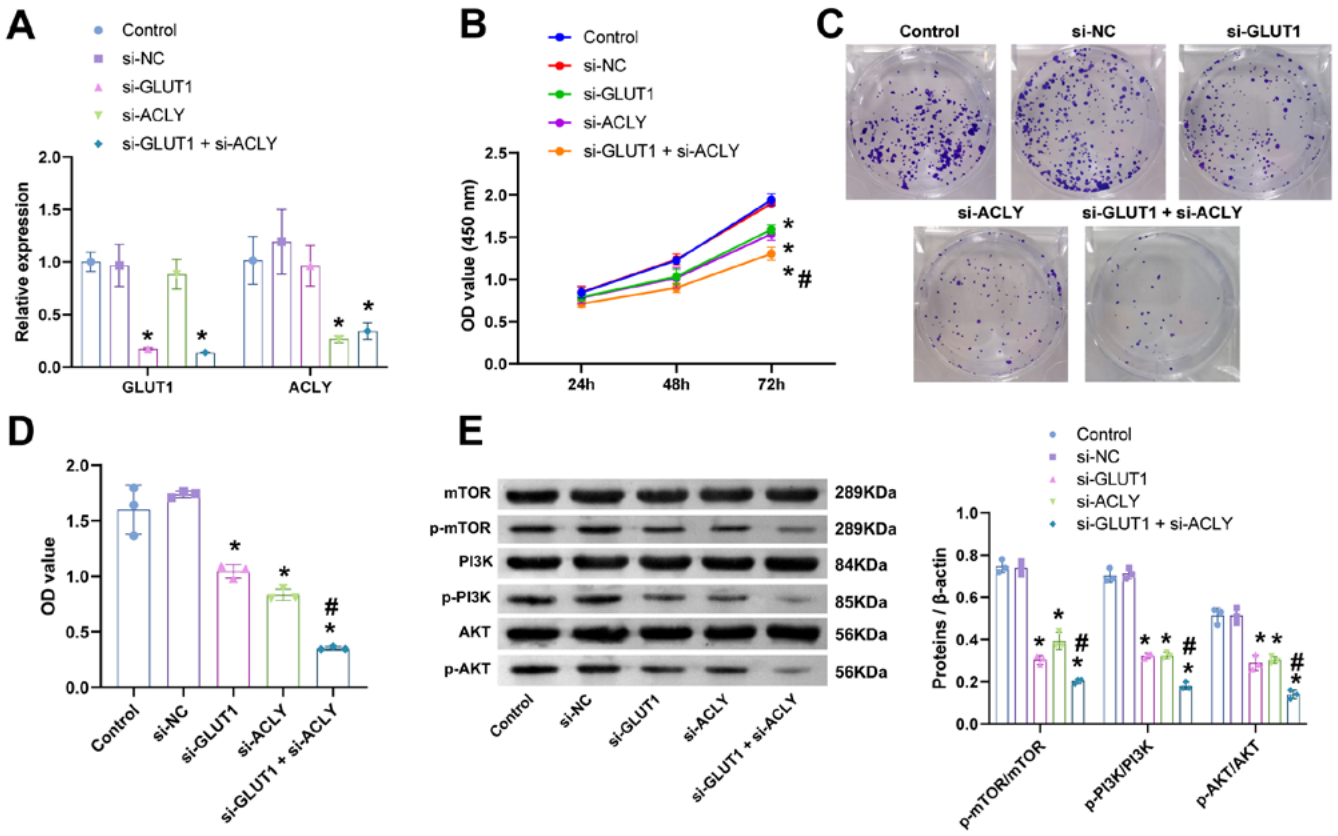

Fig. 4. GLUT1 and ACLY could inhibit the proliferation of GBC-SD cells. A. Quantitative reverse transcription polymerase chain reaction (RT-qPCR) was performed to detect the level of GLUT1 and ACLY; B. Cell Counting Kit-8 (CCK-8) was used to examine GBC-SD cell proliferation at 24 h, 48 h and 72 h; C,D. Clone formation was used to analyze the number of GBC-SD cloned cells; E. Western blot was utilized to detect the expression of proliferation-related pathway proteins (mTOR, p-mTOR, PI3K, p-PI3K, AKT, and p-AKT). Data were analyzed using one-way analysis of variance (ANOVA), followed by Tukey's post hoc test (n = 3)

*p < 0.05 compared to controls or si-NC; #p < 0.05 compared to si-GLUT1 or si-ACLY; OD – optical density; NC – negative control; GBC – gallbladder cancer; hucMSCs-exo – hucMSCs-derived exosomes.

Discussion

The understanding of clinicopathological characteristics of SC/ASC derives from studying the cases and analyzing small groups of patients. Therefore, more comprehensive studies are necessary to accurately understand SC/ASC tumors and adenocarcinoma differences. In malignant tumors of the gallbladder, the squamous differentiation incidence is at 1–12%.[6] In this study, we observed that ACLY with GLUT1 reversed the inhibition of GBC-SD cell proliferation and migration by exosomal miR-214-3p.

Exosomes are subsets of naturally occurring particles inside the cells, with notable functions during physiological and pathological conditions.[27] Recent data revealed that exosomes facilitate paracrine cell-to-cell communication via the transfer of different biomolecules.[28] Evidence points to the fact that these nanoparticles can deliver numerous biotherapeutic agents to the target cells by using different fusion mechanisms and ligand–receptor interactions.[29] Exosomes can act as biological shuttles and can even treat neurological damage.[30] The SFB-miR-214-3p exosomes suppressed apoptosis and inflammation in chondrocytes.[31] The overexpression of miR-214-3p repressed proliferation and cancer cell stemness in vitro and in vivo in squamous cell lung cancer via targeting YAP1[32] and fibroblast growth factor/MAPK signaling.[33] Han et al. suggested that miR-214-3p modulated breast cancer cell proliferation and apoptosis by targeting Survivin.[34] The miR-214-3p also interacted with TWIST1 to suppress the epithelial-to-mesenchymal transition of endometrial cancer cells.[35] In our study, exosomal miR-214-3p inhibited the proliferation and migration of GBC-SD cells and promoted their apoptosis. Exosomal miR-214-3p can reduce the activity of GBC-SD cells. This may have significant efficacy in treating the progressive development of GBC.

The ACLY is an enzyme that has recently been proven to be the key to the metabolism of cancer cells.[8,36] The ACLY is the main source of acetyl-Coenzyme A, an important precursor for fatty acid, cholesterol, and isoprenoid biosynthesis, and it is also involved in protein acetylation.[37] The activation of ACLY signaling is linked to many cancers, such as prostate cancer, lung adenocarcinoma, leukemia, glioblastoma, ovarian cancer, and liver cancer.[21] A positive expression of GLUT1 significantly predicts a poor prognosis in lung cancer patients. The GLUT1 may serve as a helpful biomarker and a potential target for the treatment strategies of lung cancer.[38] The blocking

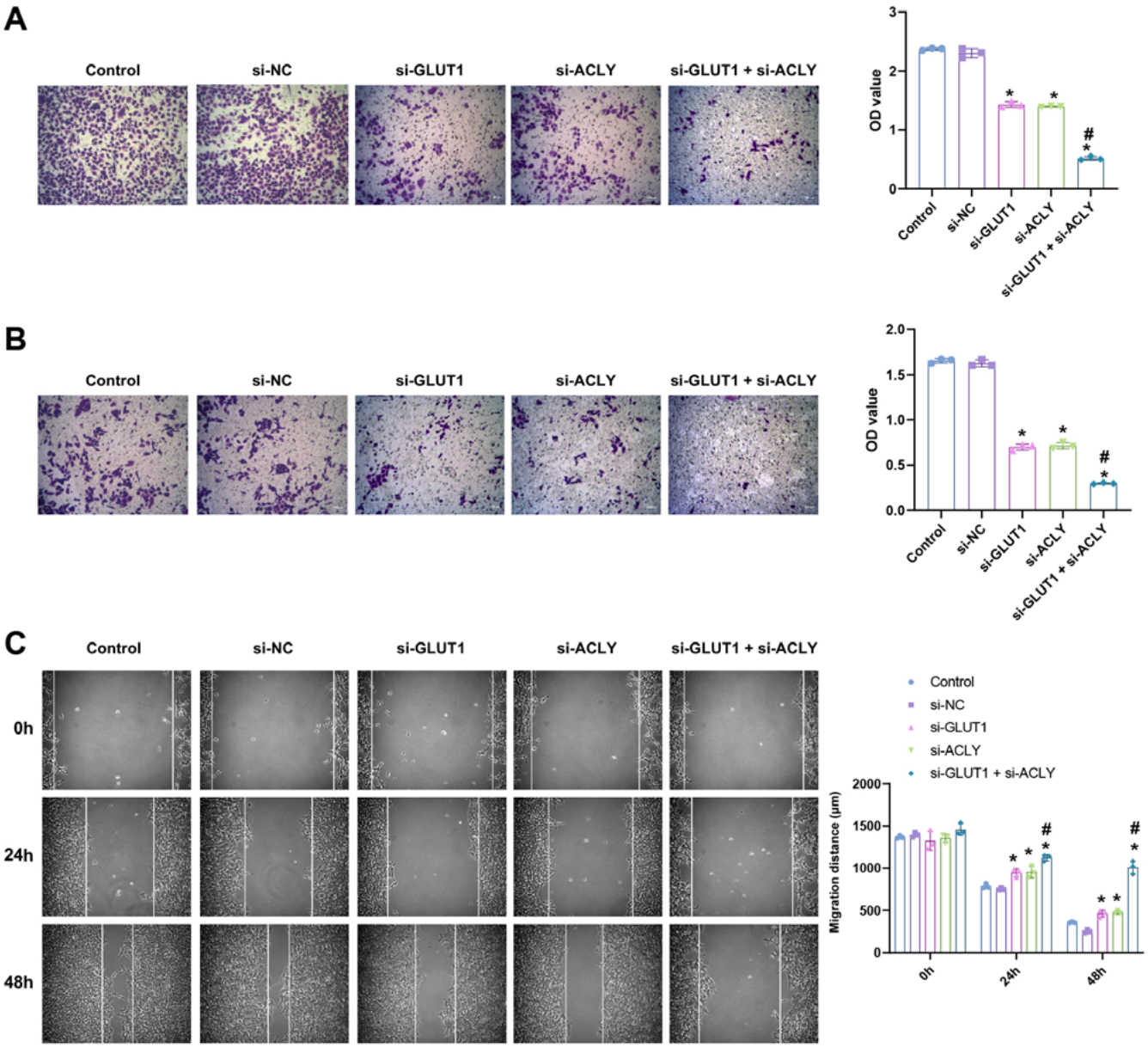

Fig. 5. GLUT1 and ACLY can inhibit the migration of GBC-SD cells. A,B. Transwell assay was used to test GBC-SD cell migration and invasion ability; C. The scratch assay was utilized to detect the migration distance of GBC-SD cells. The comparisons among multiple groups were analyzed using one-way analysis of variance (ANOVA) (n = 3)

*p < 0.05 compared to controls or si-NC; #p < 0.05 compared to si-GLUT1 or si-ACLY; OD – optical density; NC – negative control; GBC – gallbladder cancer; hucMSCs-exo – hucMSCs-derived exosomes.

of ACLY by siRNA can inhibit the Akt pathway, resulting in tumorigenicity loss in vitro. It is believed that blocking the ACLY pathway may have the potential to treat cancers. The results of this study showed that the knockdown of ACLY and GLUT1 inhibited the proliferation of GBC-SD cells and promoted apoptosis.

Limitations

It is thought that specific blocking of the GLUT1 and ACLY pathways may have the potential to treat human cancers. We will explore the effects of GLUT1 and ACLY on animal and human GBC in the future.

Conclusions

In conclusion, we found that exosomal miR-214-3p can target and inhibit ACLY. The miR-214-3p can inhibit the proliferation of GBC-SD cells. The overexpression of GLUT1 and ACLY promoted the proliferation of GBC-SD cells. In vitro experiments revealed that miR-214-3p can interfere with the activity of GBC-SD cells by inhibiting ACLY, which provided a basic theory for the treatment of GBC.

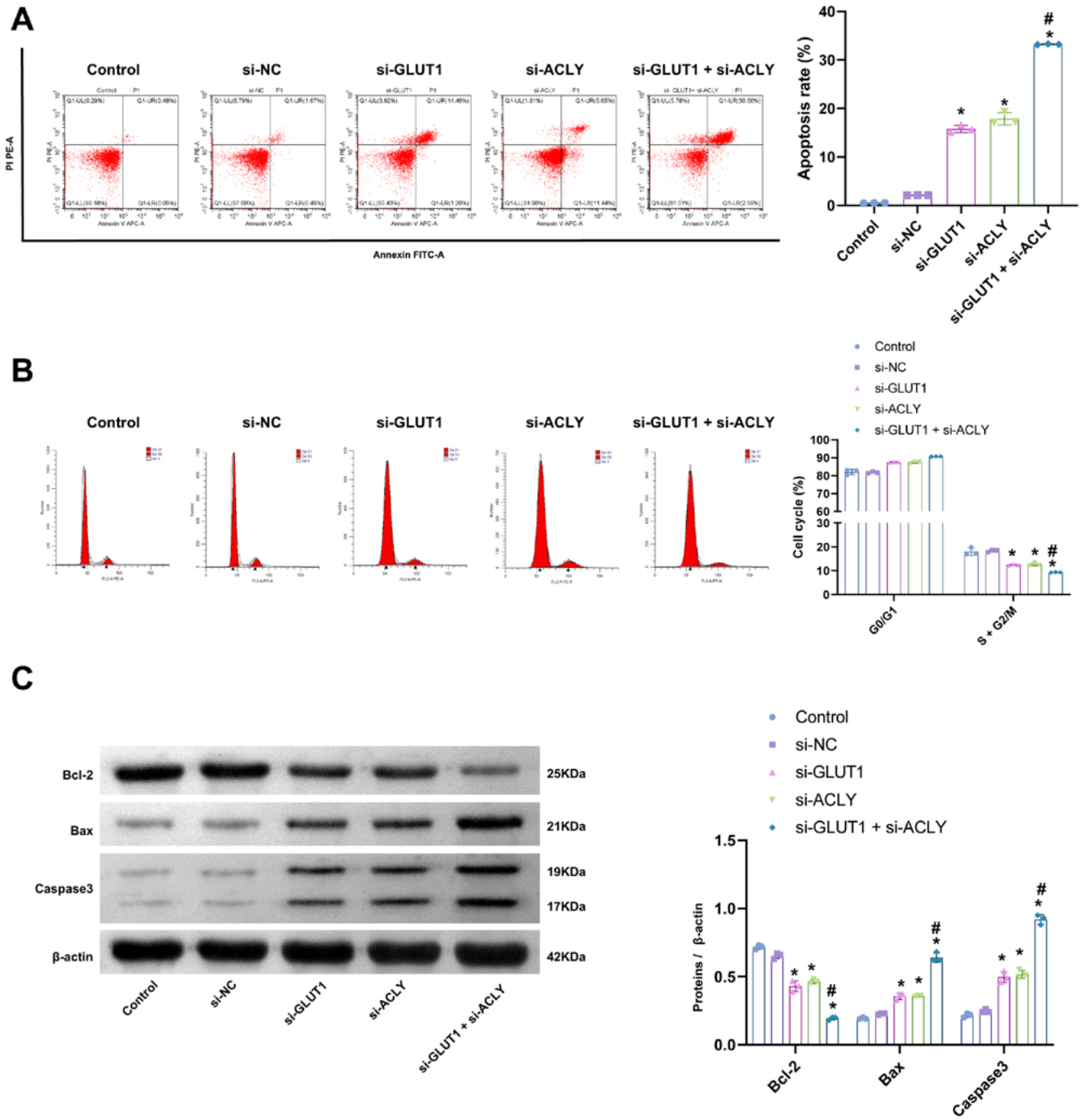

Fig. 6. GLUT1 and ACLY can promote the apoptosis of GBC-SD cells. A. GBC-SD cell apoptosis rate was promoted in the presence of GLUT1 and ACLY silencing; B. Flow cytometry was used to detect the GBC-SD cell cycle; C. Western blot was performed to detect the expression of apoptosis-related pathway proteins Bcl-2, Bax and caspase 3. Data were analyzed using one-way analysis of variance (ANOVA), followed by Tukey's post-hoc test (n = 3)

*p < 0.05 compared to controls or si-NC; #p < 0.05 compared to si-GLUT1 or si-ACLY; NC – negative control; GBC – gallbladder cancer; hucMSCs-exo – hucMSCs-derived exosomes.

Supplementary data

The supplementary materials are available at https://doi.org/10.5281/zenodo.8161958. The package contains the following files:

Supplementary Table 1. The expression of miR-214-3p.

Supplementary Table 2. The proliferation and apoptosis of GBC-SD cells.

Supplementary Table 3. miR-214-3p can regulate ACLY/GLUT1 to affect GBC-SD cells.

Supplementary Table 4. Inhibition of GLUT1 and ACLY could affect the proliferation of GBC-SD cells.

Supplementary Table 5. GLUT1 and ACLY could inhibit the migratory ability of GBC-SD cells.

Supplementary Table 6. GLUT1 and ACLY could affect the apoptosis of GBC-SD cells.

ORCID iDs

Luyao Liu https://orcid.org/0000-0001-5241-967X
Wang Xiao https://orcid.org/0009-0002-9611-3845
Zhulin Yang https://orcid.org/0009-0000-3548-7961
Qunwei Wang https://orcid.org/0009-0001-3195-5665
Jianing Yi https://orcid.org/0000-0002-3282-3285

References

1. Torre LA, Bray F, Siegel RL, Ferlay J, Lortet-Tieulent J, Jemal A. Global cancer statistics, 2012. *CA Cancer J Clin*. 2015;65(2):87–108. doi:10.3322/caac.21262
2. Sharma A, Sharma KL, Gupta A, Yadav A, Kumar A. Gallbladder cancer epidemiology, pathogenesis and molecular genetics: Recent update. *World J Gastroenterol*. 2017;23(22):3978. doi:10.3748/wjg.v23.i22.3978
3. Wernberg JA, Lucarelli DD. Gallbladder cancer. *Surg Clin North Am*. 2014;94(2):343–360. doi:10.1016/j.suc.2014.01.009
4. Mao W, Deng F, Wang D, Gao L, Shi X. Treatment of advanced gallbladder cancer: A SEER-based study. *Cancer Med*. 2020;9(1):141–150. doi:10.1002/cam4.2679
5. Hu YP, Jin YP, Wu XS, et al. LncRNA-HGBC stabilized by HuR promotes gallbladder cancer progression by regulating miR-502-3p/SET/AKT axis. *Mol Cancer*. 2019;18(1):167. doi:10.1186/s12943-019-1097-9
6. Liu L, Yang ZL, Wang C, et al. The expression of Notch 1 and Notch 3 in gallbladder cancer and their clinicopathological significance. *Pathol Oncol Res*. 2016;22(3):483–492. doi:10.1007/s12253-015-0019-4
7. Liu DC, Yang ZL. MTDH and EphA7 are markers for metastasis and poor prognosis of gallbladder adenocarcinoma. *Diagn Cytopathol*. 2013;41(3):199–205. doi:10.1002/dc.21821
8. Furuta E, Okuda H, Kobayashi A, Watabe K. Metabolic genes in cancer: Their roles in tumor progression and clinical implications. *Biochim Biophys Acta Rev Cancer*. 2010;1805(2):141–152. doi:10.1016/j.bbcan.2010.01.005
9. Osugi J, Yamaura T, Muto S, et al. Prognostic impact of the combination of glucose transporter 1 and ATP citrate lyase in node-negative patients with non-small lung cancer. *Lung Cancer*. 2015;88(3):310–318. doi:10.1016/j.lungcan.2015.03.004
10. Ganapathy-Kanniappan S, Geschwind JFH. Tumor glycolysis as a target for cancer therapy: Progress and prospects. *Mol Cancer*. 2013;12(1):152. doi:10.1186/1476-4598-12-152
11. Li Z, Zhang H. Reprogramming of glucose, fatty acid and amino acid metabolism for cancer progression. *Cell Mol Life Sci*. 2016;73(2):377–392. doi:10.1007/s00018-015-2070-4
12. Jang SM, Han H, Jang KS, et al. The glycolytic phenotype is correlated with aggressiveness and poor prognosis in invasive ductal carcinomas. *J Breast Cancer*. 2012;15(2):172. doi:10.4048/jbc.2012.15.2.172
13. Khwairakpam A, Shyamananda M, Sailo B, et al. ATP citrate lyase (ACLY): A promising target for cancer prevention and treatment. *Curr Drug Targets*. 2015;16(2):156–163. doi:10.2174/1389450115666141224125117
14. Mezheyeuski A, Nerovnya A, Bich T, Tur G, Ostman A, Portyanko A. Inter- and intra-tumoral relationships between vasculature characteristics, GLUT1 and budding in colorectal carcinoma. *Histol Histopathol*. 2015;30(10):1203–1211. doi:10.14670/HH-11-613
15. Xie S, Zhou F, Wang J, et al. Functional polymorphisms of ATP citrate lyase gene predicts clinical outcome of patients with advanced colorectal cancer. *World J Surg Onc*. 2015;13(1):42. doi:10.1186/s12957-015-0440-x
16. Kawamura T, Kusakabe T, Sugino T, et al. Expression of glucose transporter-1 in human gastric carcinoma: Association with tumor aggressiveness, metastasis, and patient survival. *Cancer*. 2001;92(3):634–641. doi:10.1002/1097-0142(20010801)92:3<634::AID-CNCR1364>3.0.CO;2-X
17. Qian X, Hu J, Zhao J, Chen H. ATP citrate lyase expression is associated with advanced stage and prognosis in gastric adenocarcinoma. *Int J Clin Exp Med*. 2015;8(5):7855–7860. PMID:26221340. PMCID:PMC4509285.
18. Amann T, Hellerbrand C. GLUT1 as a therapeutic target in hepatocellular carcinoma. *Exp Opin Ther Targets*. 2009;13(12):1411–1427. doi:10.1517/14728220903307509
19. Jiang H, Dai J, Huang X, et al. Genetic variants in de novo lipogenic pathway genes predict the prognosis of surgically-treated hepatocellular carcinoma. *Sci Rep*. 2015;5(1):9536. doi:10.1038/srep09536
20. Xiao H, Wang J, Yan W, et al. GLUT1 regulates cell glycolysis and proliferation in prostate cancer. *Prostate*. 2018;78(2):86–94. doi:10.1002/pros.23448
21. Gao Y, Islam MS, Tian J, Lui VWY, Xiao D. Inactivation of ATP citrate lyase by cucurbitacin B: A bioactive compound from cucumber, inhibits prostate cancer growth. *Cancer Lett*. 2014;349(1):15–25. doi:10.1016/j.canlet.2014.03.015
22. Galbraith L, Leung HY, Ahmad I. Lipid pathway deregulation in advanced prostate cancer. *Pharmacol Res*. 2018;131:177–184. doi:10.1016/j.phrs.2018.02.022
23. Qiu L, Wang J, Chen M, Chen F, Tu W. Exosomal microRNA-146a derived from mesenchymal stem cells increases the sensitivity of ovarian cancer cells to docetaxel and taxane via a LAMC2-mediated PI3K/Akt axis. *Int J Mol Med*. 2020;46(2):609–620. doi:10.3892/ijmm.2020.4634
24. Li K, Zhang J, Yu J, et al. MicroRNA-214 suppresses gluconeogenesis by targeting activating transcriptional factor 4. *J Biol Chem*. 2015;290(13):8185–8195. doi:10.1074/jbc.M114.633990
25. Li D, Liu J, Guo B, et al. Osteoclast-derived exosomal miR-214-3p inhibits osteoblastic bone formation. *Nat Commun*. 2016;7(1):10872. doi:10.1038/ncomms10872
26. He GN, Bao NR, Wang S, Xi M, Zhang TH, Chen FS. Ketamine induces ferroptosis of liver cancer cells by targeting lncRNA PVT1/miR-214-3p/GPX4. *Drug Des Devel Ther*. 2021;15:3965–3978. doi:10.2147/DDDT.S332847
27. Armstrong JPK, Holme MN, Stevens MM. Re-engineering extracellular vesicles as smart nanoscale therapeutics. *ACS Nano*. 2017;11(1):69–83. doi:10.1021/acsnano.6b07607
28. Hassanpour M, Cheraghi O, Brazvan B, et al. Chronic exposure of human endothelial progenitor cells to diabetic condition abolished the regulated kinetics activity of exosomes. *Iran J Pharm Res*. 2018;17(3):1068–1080. PMID:30127829. PMCID:PMC6094433.
29. Heidarzadeh M, Gürsoy-Özdemir Y, Kaya M, et al. Exosomal delivery of therapeutic modulators through the blood–brain barrier: Promise and pitfalls. *Cell Biosci*. 2021;11(1):142. doi:10.1186/s13578-021-00650-0
30. Shokrollahi E, Nourazarian A, Rahbarghazi R, et al. Treatment of human neuroblastoma cell line SH-SY5Y with HSP27 siRNA tagged-exosomes decreased differentiation rate into mature neurons. *J Cell Physiol*. 2019;234(11):21005–21013. doi:10.1002/jcp.28704
31. Lai C, Liao B, Peng S, Fang P, Bao N, Zhang L. Synovial fibroblast-miR-214-3p-derived exosomes inhibit inflammation and degeneration of cartilage tissues of osteoarthritis rats. *Mol Cell Biochem*. 2023;478(3):637–649. doi:10.1007/s11010-022-04535-9
32. Lu T, Yang Y, Li Z, Lu S. MicroRNA-214-3p inhibits the stem-like properties of lung squamous cell cancer by targeting YAP1. *Cancer Cell Int*. 2020;20(1):413. doi:10.1186/s12935-020-01506-2
33. Yang Y, Li Z, Yuan H, et al. Reciprocal regulatory mechanism between miR-214-3p and FGFR1 in FGFR1-amplified lung cancer. *Oncogenesis*. 2019;8(9):50. doi:10.1038/s41389-019-0151-1
34. Han LC, Wang H, Niu FL, Yan JY, Cai HF. Effect miR-214-3p on proliferation and apoptosis of breast cancer cells by targeting survivin protein. *Eur Rev Med Pharmacol Sci*. 2019;23(17):7469–7474. doi:10.26355/eurrev_201909_18856
35. Fang YY, Tan MR, Zhou J, et al. miR-214-3p inhibits epithelial-to-mesenchymal transition and metastasis of endometrial cancer cells by targeting TWIST1. *Onco Targets Ther*. 2019;12:9449–9458. doi:10.2147/OTT.S181037
36. Zaidi N, Swinnen JV, Smans K. ATP-citrate lyase: A key player in cancer metabolism. *Cancer Res*. 2012;72(15):3709–3714. doi:10.1158/0008-5472.CAN-11-4112
37. Mashima T, Seimiya H, Tsuruo T. De novo fatty-acid synthesis and related pathways as molecular targets for cancer therapy. *Br J Cancer*. 2009;100(9):1369–1372. doi:10.1038/sj.bjc.6605007
38. Zhang B, Xie Z, Li B. The clinicopathologic impacts and prognostic significance of GLUT1 expression in patients with lung cancer: A meta-analysis. *Gene*. 2019;689:76–83. doi:10.1016/j.gene.2018.12.006